Original scientific paper

MIXED-FLOW PUMP OPTIMISATION AND FLOW CHARACTERISTICS BASED ON THE 'DUAL CARBON' GOALS

Minjia Chen[1], Xingqi Luo[1], Wanbo Chen[2], Jianjun Feng[1], Xiaohang Wang[3,4,5]

[1]Xi'an University of Technology, Shaanxi, China
[2]Jiangxi Ganneng Co., Ltd., Nanchang, China
[3]State Key Laboratory of Hydropower Equipment, Harbin, China
[4]Harbin Electric Machinery Co., Ltd., Harbin, China
[5]Harbin Institute of Large Electrical Machinery, Harbin, China

Abstract: *Urban water supply and drainage, the shipbuilding industry, the petrochemical industry and other professional fields rely heavily on mixed-flow pumps. Enhancing the efficiency of mixed-flow pumps is crucial for achieving the 'dual carbon' goals and promote energy saving and emission reduction. In this study, the guide vane and impeller of the mixed-flow pump were optimised, focusing on its low head and effectiveness in power plants. The performance of the original and optimised pumps was then evaluated under various flow rate conditions, and their hydraulic performance was compared. Results showed that the efficiency of the optimised mixed-flow pump was improved, resulting in effective enhancement of energy loss in the pump passage. The optimised guide vane facilitated smoother water flow into the outlet pipeline, achieving energy savings, emission reduction and contributing to the realisation of the 'dual carbon' goals.*

Key words: *Mixed-flow pump, Guide vane optimisation, Impeller optimisation, Numerical simulation, Hydraulic performance*

1. INTRODUCTION

A study was proposed for the first time that China aims to achieve carbon peak in 2030 and carbon neutrality in 2060 [1]. Compared with developed countries, such as the United States and Britain, China faces remarkable challenges in terms of its economy, energy structure and utilisation rate. At present, China's carbon emissions account for 28.8% of the global total, with per capita emissions also amongst the highest. Energy conservation and emission reduction have become the main goals in various industries to realise

successfully the 'dual carbon' goals. Mixed-flow pumps find applications in diverse fields, including irrigation, drainage, flood control and water circulation systems of power stations [2]. These pumps offer advantages, such as high head, large flow and a wide efficient range. However, the mixed-flow pump is a large-scale energy-consuming equipment that consumes a considerable amount of energy, making its operating efficiency a critical factors in achieving the 'dual carbon' targets [3].

The impeller, which serves as the core component of mixed-flow pumps [4], plays a vital role in determining their performance. The design theories for mixed-flow pumps include 1D, 2D and 3D approaches. [5-7]. Both the 1D and 2D theories are based on the assumption that the impeller consists of infinitely thin and numerous blades, providing a foundation for solving the impeller's internal flow under simplified assumptions. With the continuous development of computer technology, the 3D design method has been widely used in pump impeller design. Ten et al. [8] proposed a 3D potential flow design based on a given circulation distribution. They derived the blade bone line equation from the blade boundary conditions and obtained the designed blade shape by solving the blade bone line. The flow control equation was solved using the spectral method to design the impeller. Huang et al. [9] optimised the design of mixed-flow pump impellers based on streamline load distribution and blade trailing edge angle as design parameters, and they performed numerical simulation calculations. Appropriate backloading helps to smooth the velocity gradient in the blade channel and eliminate secondary flow [10,11]. Using the 3D design platform for mixed-flow pump impellers, Hao and Shu Liang [12,13] improved the genetic algorithm and established a 3D optimisation and design system for mixed-flow pump impellers. They also explored the relationship between different blade angle deviations and the hydraulic performance of the mixed-flow pump, using both numerical simulation and model tests. The results show that when the blade rotation angle is positive, the curve moves in the direction of high flow, whereas a negative angle shifts the curve towards small flow. Several scholars at home and abroad have conducted research on the internal flow analysis of mixed-flow pumps. Muggli et al. [14] used a combined approach of steady-state and unsteady-state calculations to predict the performance of a mixed-flow pump. They found that unsteady flow simulations, which require more computational resources, are also feasible in an industrial environment and provide detailed information about the flow patterns and pressure fluctuations within the pump. The performance curves obtained from the two methods were consistent with the measured results. Moreover, the study focused on analysing the unstable flow structure of mixed-flow pumps under certain operating conditions, providing insights into abnormal flow characteristics. The results showed that under low flow conditions, unsteady calculations were better suited for analysing the unsteady flow phenomena. Saha et al. [15] created a j-groove using computational fluid dynamics (CFD) technology to investigate the causes of humps in the performance curve. They found that through experiments, it can be determined that the optimal slot shape and position have a significant effect on reducing the vortex intensity and backflow propagation in the impeller inlet area. Through angular momentum absorption owing to mixing of groove reverse flow-and swirl flow, the theoretical head of the impeller is restored [16]. Kim et al. [17] found that under the design working condition, the suction performance improved with increased blade thickness, incident angle and total pressure. Derakhshan et al. [18] focused on centrifugal pump impellers, optimising their geometry using optimisation algorithms and 3D Navier–Stokes flow solvers. The numerical results show an increase of 6.89 m in total differential pressure and a 3.59%

improvement in efficiency for the centrifugal pump. Kim et al. [19-21] conducted a multi-parameter optimisation design of the impeller and guide vane of mixed flow pumps using CFD technology. The hydraulic performance of the mixed-flow pump was taken as the objective function through an orthogonal test, optimising several variables that mutually affect each other to obtain the best hydraulic model for the mixed flow pump. The optimisation model exhibited improved head and efficiency compared with the original model. Srivastava et al. [22] adopted experimental and numerical simulation methods to correct the setting angle of the vanes by analysing the pressure distribution in the inner flow passage of the impeller. The aim was to optimise the hydraulic performance of the mixed-flow pump. The results showed that compared with the original model, the pressure distribution on the blade surface of the impeller, designed through an inverse problem approach, became more uniform, the low-pressure area was significantly reduced and overall hydraulic performance improved. Orozco Murillo et al. [23] used genetic algorithm methods for single-objective and multi-objective geometrical optimisations of jet pumps for vacuum distillation of ethanol, which is an application not deeply studied in scientific literature. These devices are particularly suitable for breaking azeotropes below atmospheric pressure at ambient temperature. The optimal design considered different working pressures, five dimensionless geometric parameters that can affect the operation of the jet pump and three performance parameters.

The research mentioned above highlights the challenges in optimising mixed-flow pump impellers due to numerous design parameters. The traditional method involves modifying the blade shape based on the designer's personal experience, which is time consuming and often fails to find the global optimal solution. Additionally, it lacks effective guidance on modifying the blade shape to improve performance. These limitations restrict designers from exploring a larger design space.

This study presents a new design method that combines the non-dominated sorting genetic algorithm (NSGA-II) with the 3D inverse problem solving design method [24]. This method effectively optimises the wrap angle distribution of the blades and guide vanes in the mixed-flow pump. The flow patterns inside the pump before and after optimisation are compared using detailed CFD analysis. This analysis helps identify the reasons for performance improvements in each component. The intelligent optimisation design system proposed in this study overcomes the limitations of traditional methods and remarkably reduces the optimisation design period for mixed-flow pumps. The Pareto solutions obtained during the optimisation process serve as references for designing high-performance mixed-flow pumps.

2. OPTIMISATION DESIGN THEORY

In this study, the pump design theory [25] and the multi-condition intelligent optimisation design technology are used to design the wrap angle of the guide vanes and blades for the mixed-flow pump [26]. In accordance with the existing data from power stations, the design parameters, such as the design flow and lift, are calculated inversely based on the requirements. The rated parameters are determined, and an initial estimation of the impeller's basic size is made. The axial flow channel of the pump is preliminarily determined by comparing and selecting similar hydraulic models with excellent performance. The optimal ratio is determined on the basis of the number of guide vanes

and impeller blades, which is determined as five blades and 11 guide vanes. The overall design scheme flow of the mixed-flow pump is depicted in Fig. 1.
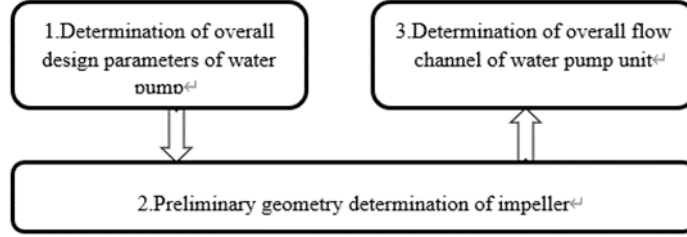

Fig. 1 Design scheme flow

In the inverse problem design method, iterative calculations are performed for the blade shape and flow field. The blade is approximated by an infinite thin vortex, and its intensity is expressed by the circumferential average angular momentum.

$$r\bar{V}_\theta = \frac{B}{2\pi} \int_0^{\frac{2\pi}{B}} r\bar{V}_\theta d\theta \tag{1}$$

where r is the radius, B is the number of blades, $\bar{V}_\theta$ is a circumferential averaged swirl velocity, and θ is the angle.

The pressure distribution in the interblade channel is determined by the partial derivative of the circumferential mean angular momentum along the streamline direction, as shown in Eq. (2).

$$P^+ - P^- = \frac{2\pi}{B} \rho W_m \frac{\partial r\bar{V}_\theta}{\partial m} \tag{2}$$

where P^+ is the static pressure on the blade's pressure surface, P^- is the static pressure on the blade's suction surface, ρ is the fluid density, W_m is the relative shaft speed and $\frac{\partial r\bar{V}_\theta}{\partial m}$ is the blade loading.

The impeller head is determined by the circumferential average angular momentum along the streamline direction as follows:

$$H_t = \frac{1}{g}\left(u_2 v_{n2} - u_1 v_{n1}\right) = \frac{\omega}{2\pi g}\left(\Gamma_2 - \Gamma_1\right) \tag{3}$$

where H_t is the theoretical head of the impeller, which consists of the dynamic head and potential head. The dynamic head is represented by the specific kinetic energy. The potential head represents the increase in position head and pressure head., ω is the angular velocity, u_n is the tangential velocity (i.e. the circumferential velocity at which the flow rotates with the impeller), v_{nn} is the absolute velocity component in the circumferential direction, Γ_n is the circulation and subscripts 1 and 2 indicate the inlet and outlet sides of the impeller, respectively. The calculation of the blade shape is the inverse problem is based

on the conditions of no-slip and no-penetration of velocity on the blade surface. The blocking effect of the blade is determined by the blade thickness parameter in the continuity equation [27]. In the 3D inverse design problem, the design parameters that can be fixed are as follows: (1) projection of the blade axis surface, (2) blade thickness, (3) number of blades, (4) speed and (5) head.

During the design process of a mixed-flow pump, the important target parameters are hydraulic efficiency η and the minimum pressure on the blade Cp_{min}. The correlation between the two parameters should be considered under maximum head, design head and minimum head conditions. Analysing the parameter changes separately for each working condition can lead to an increase in calculation complexity, low solution efficiency and difficulty in exploration due to the large number of objective functions. Therefore, the optimisation design of the core impeller components becomes a complex multi-condition optimisation problem. The development of multi-objective multi-parameter optimisation considers the influence of algorithms, geometric parameterisation and other aspects. Under multi-condition and multi-parameter solutions, the objective functions are mutually restricted, and finding the optimal solution for all the objective functions is necessary. The NSGA II [28] has shown good applicability in multi-objective, non-continuous and nonlinear optimisation problems. The optimisation data are dimensionally reduced by converting the target function of head and efficiency, as shown in Eq. (4). The functional relationship is then differentiated to find the optimal solution, as shown in Eq. (5).

$$
\begin{aligned}
ef &= (\eta_1, \eta_2, \eta_3) \\
p &= (Cp_{min,1}, Cp_{min,2}, Cp_{min,3})
\end{aligned}
\tag{4}
$$

$$
\begin{aligned}
d_{VE}(ef_i, ef_{Des}) &= (\sum_{j=1}^{n} \left| \eta_j - \eta_{Des} \right|^2)^{\frac{1}{2}} \\
d_{VP}(p_i, p_{Des}) &= (\sum_{j=1}^{n} \left| (Cp)_{min\,i,j} - (Cp)_{min\,Des,j} \right|^2)^{\frac{1}{2}}
\end{aligned}
\tag{5}
$$

where $n=1,2,3$ represent working conditions 1, 2 and 3.

This study establishes an intelligent optimisation design system that combines CAD and CFD, improving the shortcomings of traditional design methods. Fig. 2 depicts a flow chart for the intelligent optimum design of overcurrent components. Overall, the traditional design method is cumbersome and cannot effectively consider the simultaneous improvement of performance under multiple operating conditions. The optimisation problem has many constraints, objective functions and unknown feasible domains in the design space. The advantage of the proposed design method is the dimension reduction of optimisation problem data through objective function conversion, laying a foundation for efficient solution of the optimisation problem. It reduces human resource consumption and improves impeller design through computer self-recycling calculation. However, this method requires a high computational speed and is only applicable to the optimal design of impeller blades and guide vanes of fluid machinery, with certain limitations for the design of other overflow components (such as suction chamber, volute, etc.). The efficiency of the mixed-flow pump designed using this method is obviously improved and meets design expectations. It has been successfully implemented in production. This

method also reduces the effect caused by a large number of objective functions, resulting in low solution efficiency and difficulty in effective search.
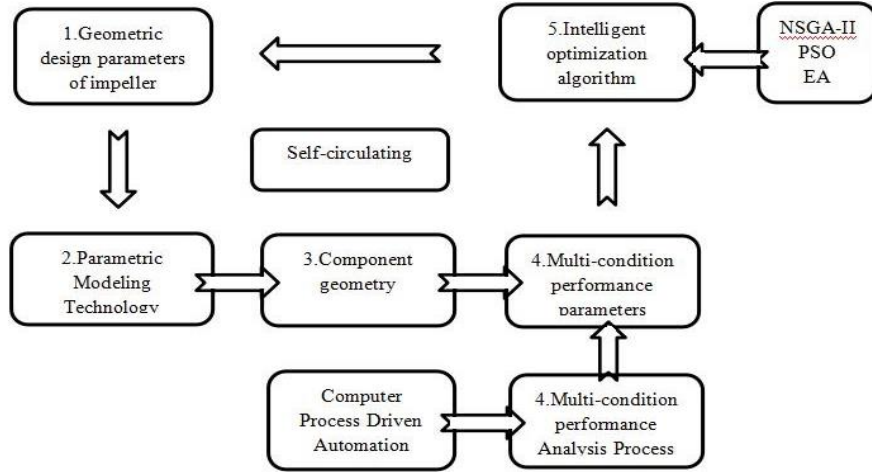

Fig. 2 Flow chart for intelligent optimum design of overcurrent components

3. PHYSICAL MODEL OF A MIXED-FLOW PUMP

3.1 Geometric model

The impeller blades, guide vanes and other overflow components of the mixed-flow pump are modelled using UG software to precisely replicate the actual shape of the pump and reduce geometric errors. Fig. 3 shows a 3Dl model of the pump. Fig. 4 depicts the geometrical modifications of the impeller vanes and movable guide vanes. The key parameters of the mixed-flow pump are listed in Table 1. In this study, numerical simulation analysis is conducted for the mixed-flow pump model before and after optimisation under low, design and large flow conditions. Table 2 shows specific parameters for the three conditions. Fig. 5 shows the impeller model of the pump.
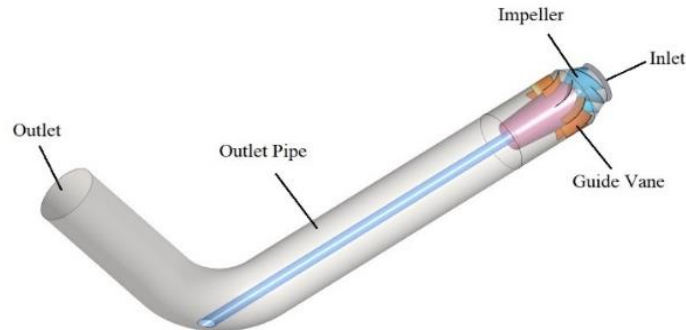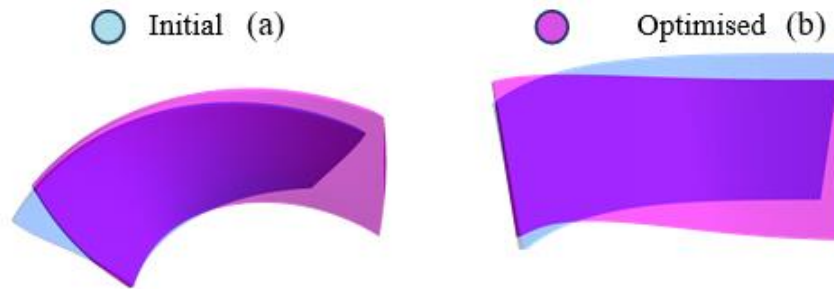

Fig. 3 Mixed-flow pump diagram

Fig. 4 (a) Blade and (b) guide vane

Table 1 Design parameters of the pump

Parameter	Value
Rated speed n (r/min)	2325
Number of impeller blades	5
Diameter of the impeller (mm)	430
Number of guide vane blades	11

Fig. 5 Model of a mixed-flow pump's impeller

3.2 Numerical calculation settings

The computational domain is divided into grids using CFD ICEM to minimise numerical calculation errors and accurately simulate the internal flow of each overflow component in the mixed-flow pump. Fig. 6 depicts the grid around impeller blades and movable guide vanes. The total number of grid nodes for the mixed-flow pump is 3.73 million. A shear stress transport turbulence model is selected as the turbulence model [29]. An automatic wall-proximity treatment is used, and the y+ value on the blade surface is kept below 30 to adapt to the turbulence model. Table 2 shows the control equation and boundary conditions. The convergence criterion for calculating convergence conditions is set such that the residual value is less than 10^{-4}.
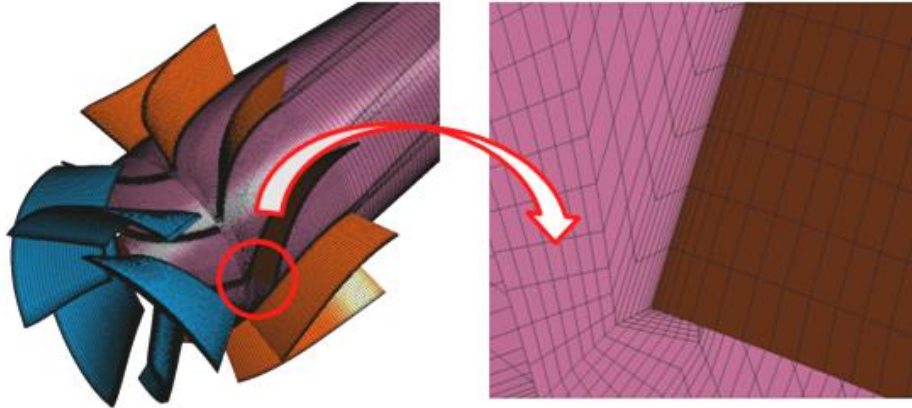
Fig. 6 Diagram of a mixed-flow pump

Table 2 Boundary conditions

CFD solver	ANSYS CFX
Inlet	Total pressure 5% turbulence intensity
Outlet	Flow
Boundary details	Smooth, no-slip
Divergent method	Second-order
Turbulence	Shear stress transport
Convergence control	$\leq 10^{-4}$

3.3 Selection of calculation conditions

The primary objectives of this study are to investigate the change in the internal flow field and the performance of the mixed-flow pump with different design schemes before and after optimisation under different operating conditions. Numerical simulation calculations and analysis are conducted for low, design and large flow conditions. Table 3 presents specific parameters for the three conditions.

Table 3 Parameters of experimental conditions.

Number	Condition	Q (m^3/s)
Q_1	Low flow rate condition	9.5
Q_2	Design flow rate condition	10.8
Q_3	Large flow rate condition	12.5

4. ANALYSIS OF OPTIMISATION RESULTS

4.1 Selection of calculation conditions

Fig. 7 depicts a performance curve comparison between the initial and optimised models. As shown in Fig. 7(left), the optimised model outperforms the initial model under the selected calculation conditions in terms of efficiency, with an increase of approximately 3%. As depicted in Fig. 7(right), the head of the optimised model is significantly higher compared with the initial model. During the transition from design to high flow conditions, neither the optimised flow-head curve [30] nor the flow-efficiency curve [31] shows any significant steep drop. Under the design conditions, the optimised head and efficiency are increased by 18.5% and 2.6%, respectively, compared with the original model. These findings indicate a remarkable improvement in the external characteristics of the optimised mixed-flow pump, aligning well with the goal of 'dual carbon' and improving energy utilisation.
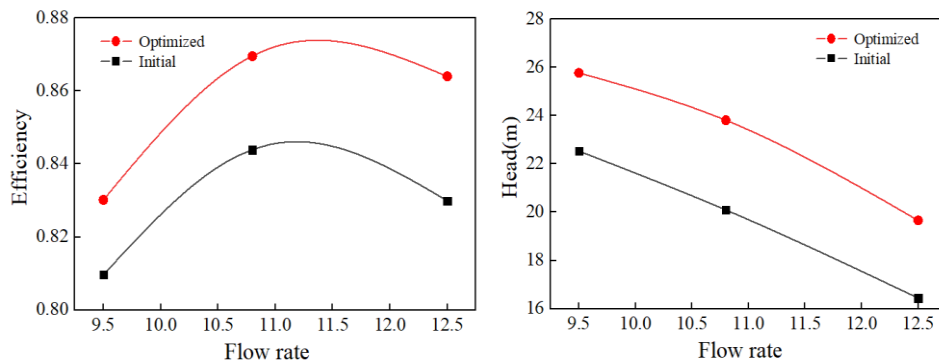

Fig. 7 Comparison of efficiency (left) and comparison of head (right)

4.2 Flow field analysis

The main flow lines of the impeller and guide vanes are depicted in three dimensions in Fig. 8 to investigate the flow conditions of the mixed-flow pump before and after optimisation under various operating conditions [32]. This figure provides insights into the variation rules of the internal flow field.

Under the small flow condition, the flow lines of the initial mixed-flow pump exhibits disorderliness near the hub at the inlet edge of the impeller components and near the pressure surface at the wheel edge. The streamline at the guide vane inlet presents a chaotic situation with certain instability and vorticity structure. The streamline at the trailing edge of the guide vane outlet disperses throughout the entire space, and the streamline inside the guide vane undergoes remarkable changes and constantly develops rearward. The whole streamline is disordered, with the presence of eddy structures. These eddies can cause flow path blockage, resulting in energy loss and performance degradation of the pump. By contrast, the results achieved after optimisation show remarkable improvements in the impeller's streamline disorder, reduction in vortex structures and stabilisation of the flow pattern at the guide vane. This leads to reduced energy loss and increased pump efficiency.

At the design condition, the streamline of the mixed-flow pump before and after optimisation tends to be smoother as flow increases. The vortex structure continues to decrease, and some vortex structures gradually disappear. The analysis shows that under the design working condition, the optimised guide vane outlet streamline is gentler compared with the initial model, the flow pattern is stable and energy loss is reduced. When operating under large flow conditions, vortex structures are generated in the guide vane channel in the initial model, affecting the water flow. However, after modification, the impeller and guide vane channels can maintain stability, with a reduction in the number and size of vortex structures to some extent.

The research findings indicate that, before optimisation, the flow becomes more unstable and the streamline becomes more turbulent as the mixed-flow pump operates further away from the design working condition, particularly at lower flows. However, the optimised mixed-flow pump shows a gradual stabilisation of the flow pattern under small flow conditions, effectively suppressing the occurrence of vortex structures. As the working conditions reach the design and large flow conditions, the flow in the impeller and guide vane further improves. The decrease in the dissipation rate of energy and the increase in unit efficiency are further manifestations of the improvement in internal flow.
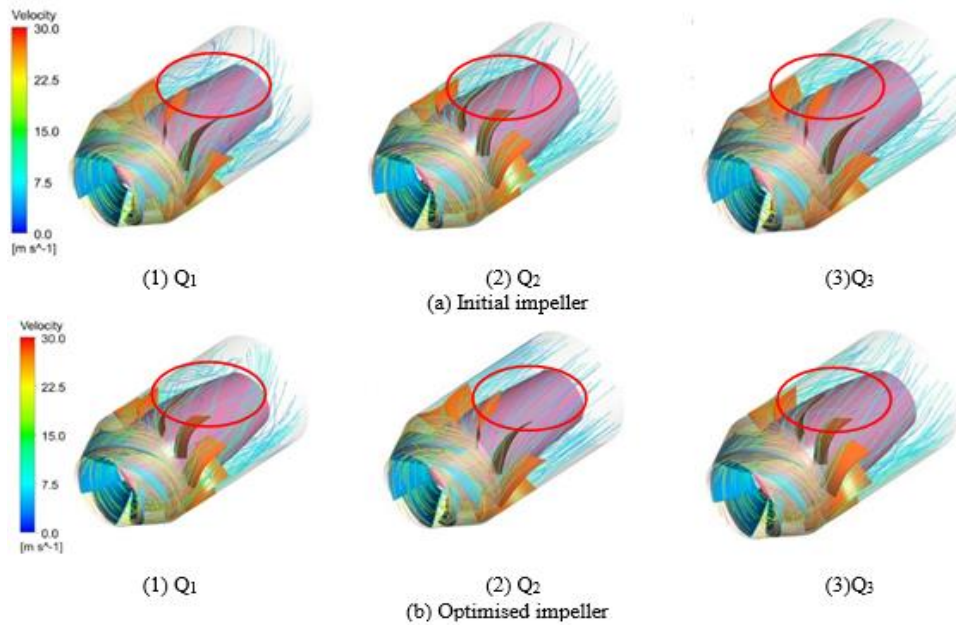

Fig. 8 Comparison of efficiency (a) and comparison of head (b)

The internal flow pattern of the pump before and after optimisation is better compared and optimised. Fig. 9 depicts segments of the streamline at the guide vane and impeller, showing the mixed flow pump's streamline distribution under design conditions. The analysis shows that the streamline near the guide vane hub is disordered before optimisation. The streamline distribution becomes uniform after optimisation, with no vortex generation. Consequently, flow separation becomes difficult, hindering the

occurrence of cavitation. The operation efficiency of the mixed-flow pump has been optimised and enhanced to some extent, and adverse flow, such as turbulence, has been reduced.
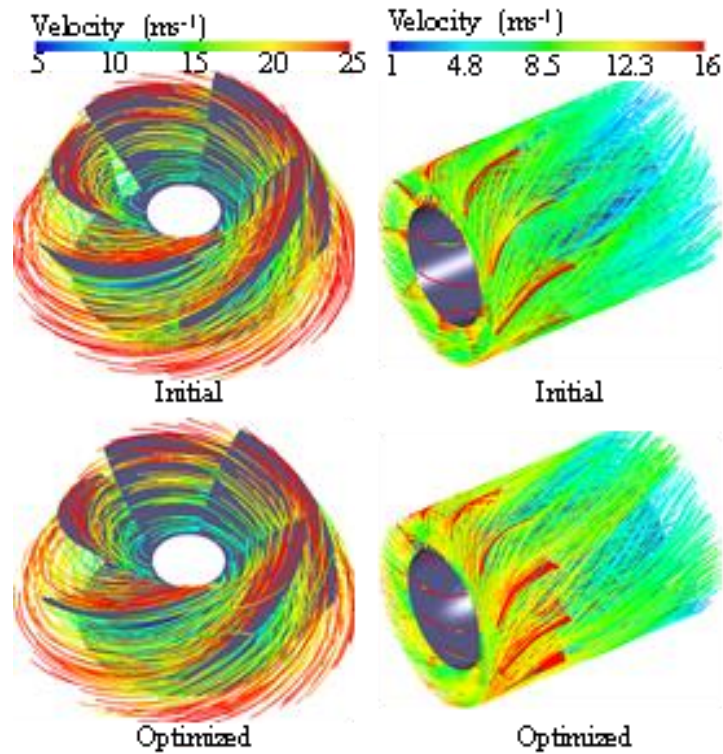

Fig. 9 Streamline distribution of impeller and guide vane

Fig. 10 shows the distribution of turbulent kinetic energy at 30%, 50% and 70% of the guide vane's cylindrical development surface to better contrast the pump's internal flow characteristics [33]. Turbulent kinetic energy indicates the development or attenuation of turbulence in time and space, and serves as a symbol for flow stability. After optimisation, the distribution of turbulent kinetic energy under small flow conditions undergoes slight changes, with a decrease in the turbulent kinetic energy in the guide vane channel. Under the pre-optimised design flow and large flow conditions, a high-intensity turbulent concentration area exists at the back of the guide vane. However, the range of high turbulent kinetic energy distribution range in the guide vane channel narrows significantly after optimisation.
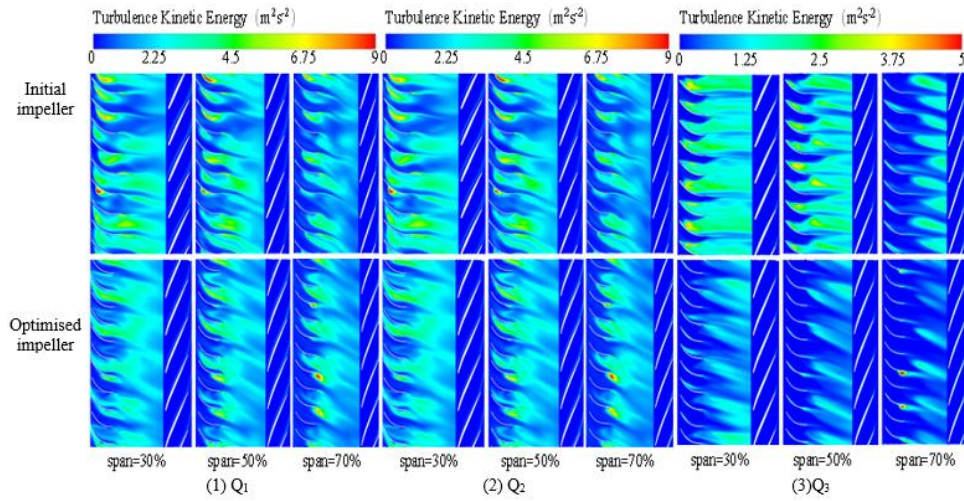
Fig. 10 Comparison of turbulence kinetic energy

Fig. 11 shows the velocity distribution at the hub flow surface, intermediate flow surface and rim flow surface in the impeller after optimisation. The flow velocity increases gradually from the hub to the rim. Under the designed operating conditions, no vortexes exist near the impeller blade in the flow passage. The streamlines are uniformly distributed, enabling stable flow into the guide vane. When the mixed-flow pump operates at a large flow, the flow path of the blade remains stable. However, a small high-speed area is generated at the blade's leading edge and end with an increase in flow, leading to energy dissipation. In summary, no adverse flow phenomena, such as impingement and backflow [34], are found near the optimised impeller blade. The inner flow lines of the impeller are smooth, vortex-free structures are generated and the flow state is good, achieving the expected optimisation results.
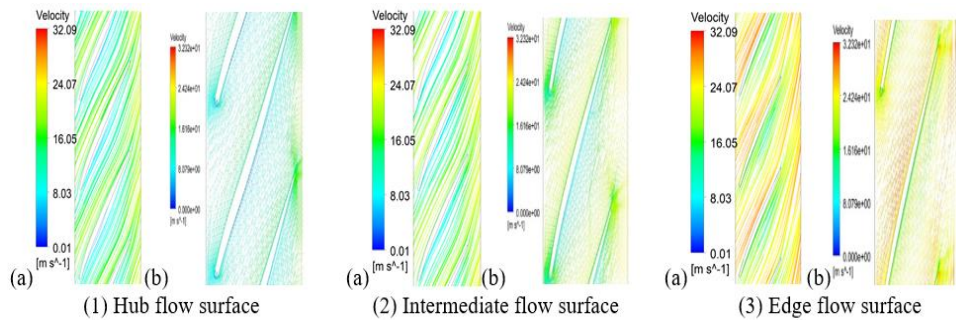

(1) Hub flow surface   (2) Intermediate flow surface   (3) Edge flow surface

Fig. 11 Streamline distribution in impeller blades (a) Optimised design conditions and (b) optimised large conditions

Fig. 12 shows the internal flow chart of the outlet pipe before and after optimisation. Water flows from the guide vane to the outlet pipe, as shown by the results. The low-speed zone at the inlet end of the outlet pipe has significantly improved, with a uniform streamline distribution and reduced eddy currents. The outlet pipe's flow rate in the mixed-flow pump is relatively slow before optimisation under design conditions, resulting in a decrease in overall efficiency. However, the outlet pipe exhibits a steady and uniform flow rate without evident speed changes after optimisation, resulting in better outlet performance.
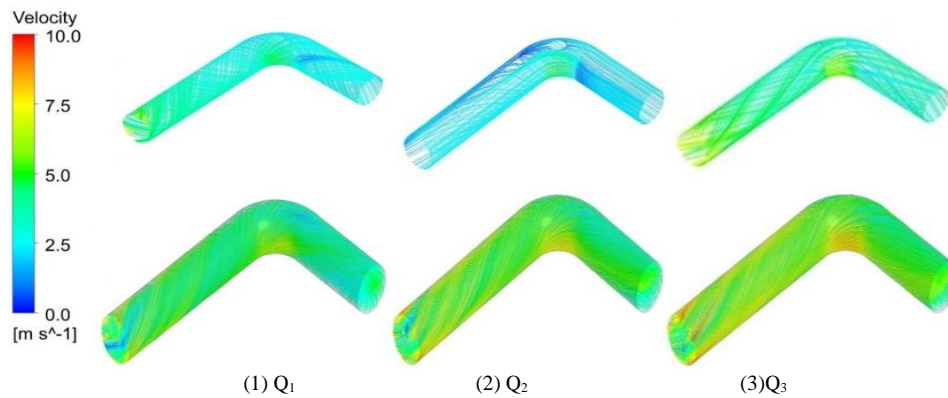

(1) Q_1 (2) Q_2 (3) Q_3

Fig. 12 Streamline distribution in impeller and guide vane

4.3 Pressure distribution

Figs. 13 and 14 show the static pressure distribution of the impeller blades of the mixed-flow pump before and after optimisation for pressure and suction. The pressure on the pressure surface of the impeller blade increases towards the wheel rim, reaching its maximum at the rim and its lowest value at the inlet of the pressure surface. The pressure distribution around the blade's middle region is greater compared with the rest of the wheel. This difference may be attributed to the longer wing on the wheel rim, which performs more work and generates higher pressure values. The suction surface and pressure surface exhibit distinct pressure change patterns. On the suction surface, the pressure gradually increases from the inlet to the outlet of the blade, with the maximum pressure occurring at the outlet. As the flow rate increases, the maximum pressure value gradually decreases. Prior to optimisation, localised low-pressure zones appeared at the blade's inlet edge, indicating the potential occurrence of vortexes in that region. After optimising the mixed-flow pump, the extent of low pressure at the blade's inlet edge gradually decreases. The suction surface of the blade experiences the minimum pressure value, whereas the pressure surface exhibits the maximum pressure value. The pressure gradient on the blade's surface is small, resulting in a relatively uniform pressure distribution along the working surface. This observation indicates that the flow channel through the blade after optimisation is better distributed and yields improved performance compared with the flow channel before optimisation.
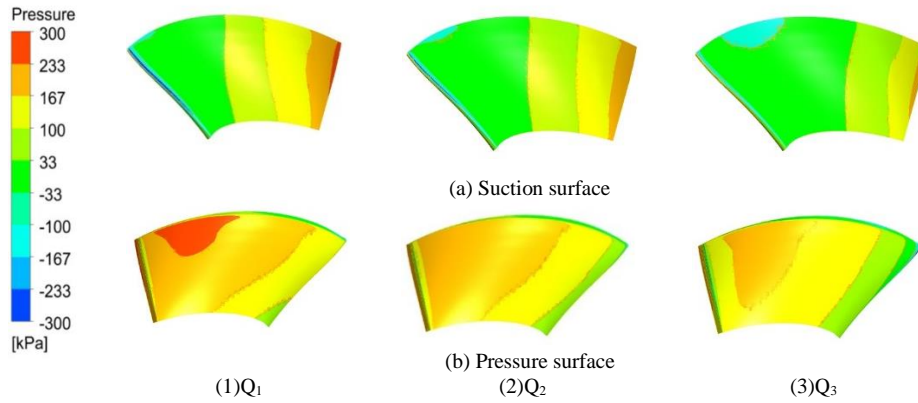
Fig. 13 Initial blade static pressure distribution (a) Suction surface and (b) Pressure surface
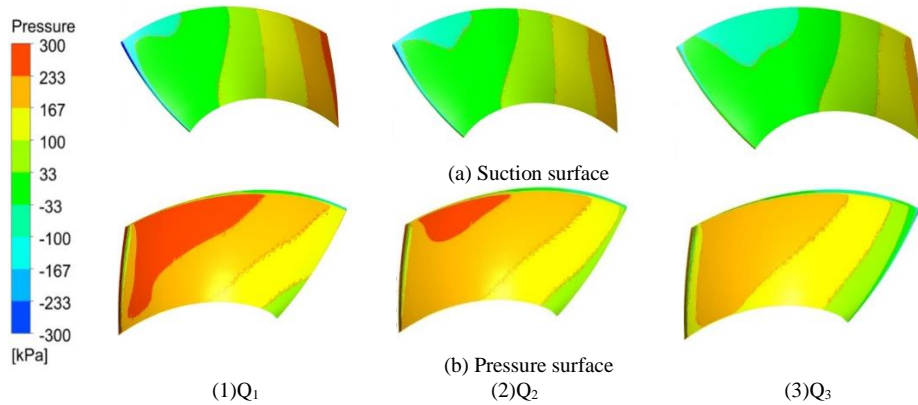

Fig. 14 Optimised blade static pressure distribution (a) Suction surface and (b) pressure surface

Figure 15 shows the pressure distribution of the impeller under design flow conditions and high flow conditions. The optimisation process eliminated low-pressure zones on the blades. The flow remains smooth without remarkable large-scale flow separation. Under the designed flow conditions, the pressure distribution across the whole impeller blade is uniform, with no apparent sudden changes in pressure. This observation demonstrates that the impeller exhibits good hydraulic performance during operation after optimisation. Fig. 16 illustrates the internal pressure distribution in the outlet pipe of the mixed-flow pump under a low flow rate conditions following optimisation. The analysis shows that the optimised pump's outlet exhibits a continuous flow without any noticeable pressure variation areas, indicating a stable overall pressure distribution. This indicates that the device effectively conveys fluid, and the optimised mixed-flow pump demonstrates favourable flow characteristics under conditions of low flow. The outlet pipe should be designed to minimise pressure pulsations, which can effectively mitigate cavitation.
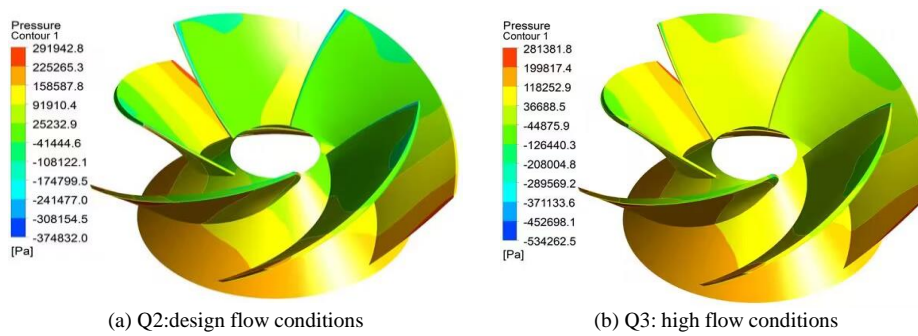
(a) Q2:design flow conditions   (b) Q3: high flow conditions

Fig. 15 Optimised pressure distribution inside the impeller (a) design flow conditions and (b) high flow conditions

Fig. 16 Pressure distribution in the outlet pipe

5. COMPARISON OF CFD NUMERICAL SIMULATION RESULTS WITH ACTUAL EXPERIMENTAL RESULTS

In accordance with the high-precision CFD analysis results, the flow line distribution in the runner of the pump developed for the project is found to be reasonable, with a good flow pattern and smooth flow in the outlet pipe without any noticeable shedding. These results indicate that the unit exhibits improved hydraulic efficiency and stability, meeting the service requirements of the power plant. The designed pumps have been successfully manufactured, installed and put into operation. Fig. 17 provides a schematic of the main components at the installation site.

Fig. 17 Field component schematics: Impeller (left) and painted guide vane body (right)

Following the installation of the optimised mixed-flow pump, several tests were conducted on both the modified and unmodified pumps under the same design conditions (i.e. design flow is 10.8 m^3/s) as used in the CFD numerical simulation. A comparison revealed that the actual efficiency of the mixed-flow pump before renovation was 82.12%, whereas the actual efficiency after renovation was 89.97%. This represents a 7.85% increase in efficiency. In the numerical simulation results, the efficiency of the mixed-flow pump before modification was predicted to be 84.08%. The efficiency of the modified mixed-flow pump was estimated to be 87.1%, resulting in a 3.02% improvement in efficiency. Although some errors were observed between the numerical simulation and actual experimental values, the overall trend of efficiency improvement was in good agreement. Table 4 provides a comparison of the efficiencies.

Table 4 Efficiency comparison

	Initial efficiency	Optimised efficiency
Numerical simulation	84.08%	87.1%
Actual testing	82.12%	89.97%

Several factors contribute to the deviation between the predicted values from numerical simulation and the experimental values: 1) During the process of establishing the geometric model for the computational domain, some reasonable simplifications were made. Certain parts of the mixed-flow pump were treated to promote convergence during grid division and ensure grid quality. 2) The numerical simulation only predicts the hydraulic efficiency in the fluid calculation area, considering only hydraulic losses within that region. However, the actual mixed-flow pump experiences additional losses, such as leakage loss and mechanical loss, which are not accounted for in the numerical simulation. 3) Differences exist between the turbulence model used in the numerical simulation and the actual turbulent flow in the actual pump.

In summary, the optimisation and renovation of the water pump resulted in an overall improvement in its performance, which aligned with the actual on–site conditions and achieved the desired effect. All three remaining pumps in the project were successfully renovated and put into operation.

6. ANALYSIS OF THE ACTUAL OPERATION EFFECT

Operational testing on both the initial and optimised mixed-flow pumps under different test conditions, including two turbine two pump technology, two turbine three pump technology and two turbine four pump technology [35]. Fig. 18 provides a schematic of the operation under these test conditions. In accordance with the operation data obtained from the DSC system, energy efficiency analysis was performed to evaluate the effect of optimisation before and after modification. Statistical calculations were conducted on the operation data of the backup pump before and after modification, in combination with real-time operation data obtained from the power plant. Energy-saving analysis was then performed on the circulating pump system.
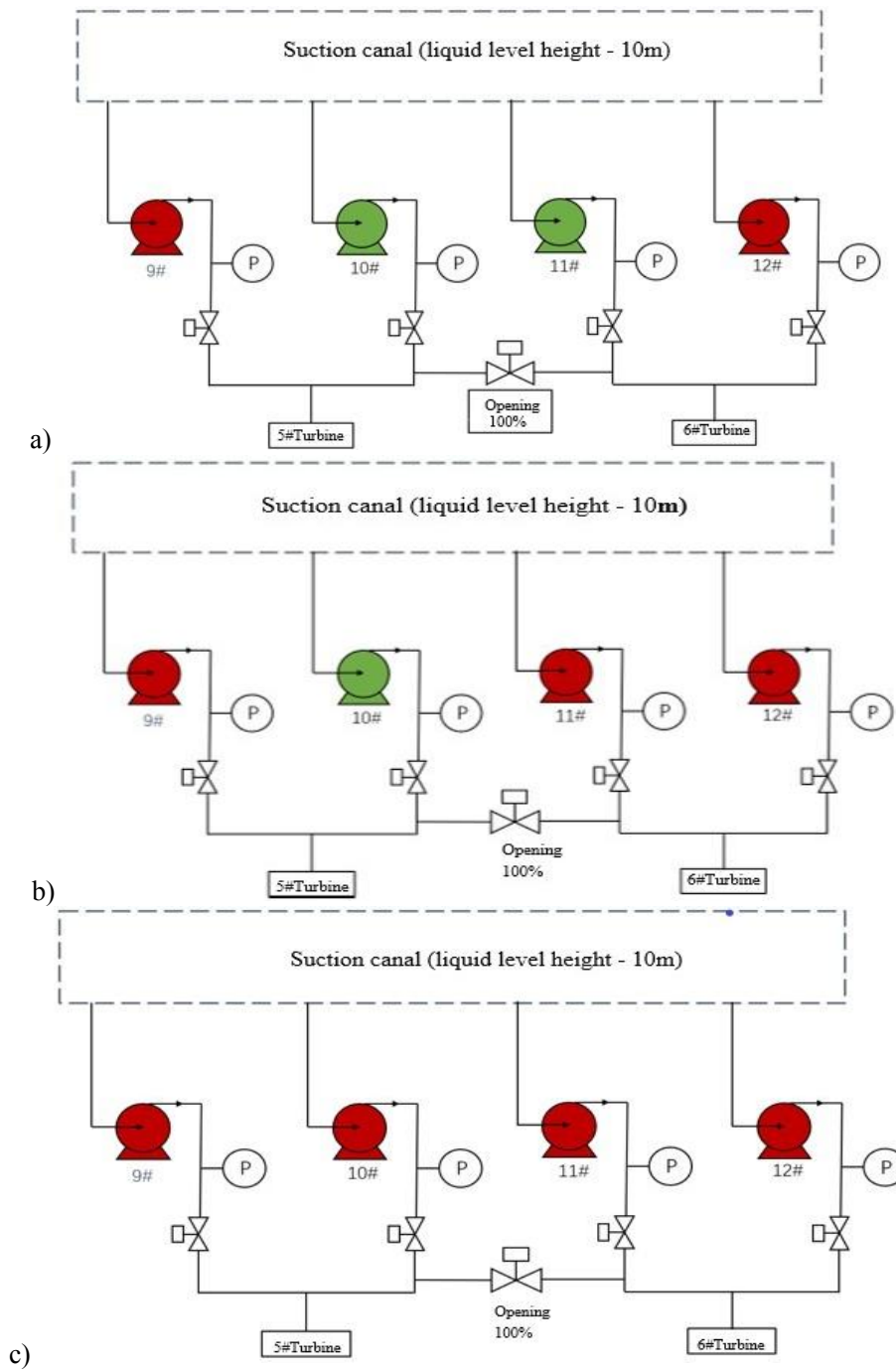
a)

b)

c)

Fig. 18 Test conditions: a) two turbine two pump technology; b) two turbine three pump technology; c) two turbine three pump technology

Table 5 summarises the retrofitting effects of the circulating pump under different operation modes. The comparison results show that the head of the new pump is higher than that of the old pump when comparing the operation data before and after modification. The head of the modified pump is adjusted to match the head of the old pump based on the performance curve. At this time, the flow rate of a single pump increases by 3.05%, 2% and 0.7%. The flow rate of the modified pump is slightly higher than before. In accordance with the performance curve, the power will be reduced, further improving the energy-saving rate. The efficiency improvement rates of the water pump after modification are found to be 15.3%, 11.97% and 7.19% by calculating the efficiency of water pump through head, flow and current, respectively. The energy-saving rate can reach 8% when the flow rate and pressure remain consistent with those before modification, indicating that an 8% energy-saving rate can be achieved through efficiency improvement. From this perspective, the pump's performance meets the expected target.

Table 5 Summary of circulating pump transformation effect under different operation modes

Operating mode	Initial			Optimised		
	Flow [m^3/h]	Head [m]	Efficiency	Flow [m^3/h]	Head [m]	Efficiency
(a)A	47656.	17.1	73.60%	41573	21.4	86.60%
(b)B	44300.	20.2	80%	41160	22.5	89.70%
(c)C	38160	24.8	83.97%	36215.	26.1	90%
Operating mode	Optimised	Data comparison		
	Same head flow [m^3/h]	Energy saving rate	Lift rate of head flow	Efficiency improvement
(a)A	49113	5.06%	3.05%	15.30%
(b)B	45193	7.30%	2%	11.97%
(c)C	38459	7.40%	0.70%	7.19%

7. CONCLUSIONS

This study focused on optimising and renovating a mixed-flow pump to align with 'dual carbon' goal. A novel mixed-flow pump design method was proposed, Incorporating an intelligent optimisation design system that combined CAD and CFD. The guide vane and blade were optimised using the3D inverse problem solving design. The effects of modification on the pump's performance were investigated, analysing the initial and optimised mixed-flow pumps under low, design and large flow conditions. The main conclusions are as follows:

(1) This study utilised the 3D inverse problem solving design method as the foundation for designing the mixed-flow pump to optimise the performance objective function under multiple working conditions and parameters. This method was supplemented by the NSGA-II and data dimensionality reduction. The combination of these techniques established an intelligent optimisation design system that effectively addressed conflicting objective functions and resulted in a better performance improvement of the optimised mixed-flow pump.

(2) The overall efficiency increased by 3.2% following the optimisation and modification of the mixed-flow pump, and the head was raised by 3.5 m. This enhancement remarkably expanded the stable working range of the unit, effectively achieving energy-saving and emission reduction goals. The process reduced energy consumption and improved the energy utilisation ratio, contributing to improved efficiency and overall performance.

(3) After the optimisation modification, the impeller and guide vane flow channels exhibited a significant reduction in vortex structure. The flow pattern became more stable, leading to the absence of obvious pressure pulsations in the outlet pipe. The pressure distribution became well-distributed, effectively reducing the occurrence probability of cavitation and prolonging the service life of the unit. These modifications contributed to improved reliability and performance.

(4) The study revealed that the optimised mixed-flow pump experienced a significant decrease in turbulent energy by comparing the turbulent energy variation laws in the flow channels of the guide vane and impeller. This reduction effectively reduced energy losses caused by pulsations, resulting in an overall performance improvement of the mixed-flow pump. Furthermore, these improvements contributed to the low-carbon transformation of energy, aligning with the objectives of the 'dual carbon' strategy.

(5) The results aligned with the numerical simulation outcomes through testing and comparing the actual mixed-flow pump installed and put into operation, confirming the achievement of expected results. The optimised mixed-flow pump demonstrated significant improvements in efficiency, energy savings and other relevant aspects, reflecting the effectiveness of this optimisation process. Additionally, all the remaining three pumps in the project were successfully revamped and put into operation.

REFERENCES

1. Yu, S., Sun, Y., Hu, X., 2022, *Research on the improvements of China's renewable energy policy system under the dual carbon goals*, J. Beijing Inst. Tech., 24(4), pp. 93–102.
2. Naresh, B., Krishna, P., Deepak, N.S., Prasanna, P.L., 2019, *Design and Analysis of Mixed Flow Pump Impeller*, International Journal of Trend in Scientific Research and Development, 3(3), pp. 1180-1184.
3. Sung K., Yong-In, K., Jin-Hyuk, K., Young-Seok, C., 2020, *Design optimization for mixed-flow pump impeller by improved suction performance and efficiency with variables of specific speeds*, Journal of Mechanical Science and Technology, 34(6), pp. 2377-2389.
4. Jun-Won, S., Hyeon-Mo, Y.,Yong-In, K., Kyoung-Yong, L., Jin-Hyuk, K., Won-Gu, J., Young-Seok, C., 2019, *Multi-objective optimization of a high efficiency and suction performance for mixed-flow pump impeller,* Engineering Applications of Computational Fluid Mechanics,13(1), pp. 744-762.
5. Shi, W., Zhang, Y., Xiao, Y., Zhou, L., 2019, *Research status of pump hydraulic design methods*, Journal of Nantong University (Natural Science Edition), 18(4), pp. 1–7.
6. Yongxue, Z., Long, C., Xin, Z., 2013, *Hydraulic design and BVF diagnosis of high efficiency centrifugal pump*, Journal of Drainage and Irrigation Machinery Engineering, 31(6), pp. 479-483.
7. Shuanbao, J., Yongsheng, W., Jiangming, D., 2012, *Three-dimensional design and numerical experiment of mixed-flow waterjet with CFD*, Journal of Harbin Engineering University, 33(10), pp. 1223–1227.
8. Tan, C.S., Hawthorne, W.R., McCune, J.E., Wang, C., 1984, *Theory of blade design for large deflections: Part II—annular cascades*, J. Eng. Gas Turbines Power, 106(2), pp. 354–365.
9. Huang, R., Luo, X., Ji, B., Wang, P., Yu, A., Zhai, Z., Zhou, J., 2015, *Multi-objective optimization of a mixed-flow pump impeller using modified NSGA-II algorithm*, Science China technological sciences, 58, pp. 2122-2130.
10. Shaheed R., Mohammadian A., Yan X., 2021, *A Review of Numerical Simulations of Secondary Flows in River Bends*, Water, 13(7), 884.

11. Tajnesaie, M., Jafari, N.E., Barati, R., Azhdary, M.M., 2020, *Performance comparison of four turbulence models for modeling of secondary flow cells in simple trapezoidal channels*, ISH Journal of Hydraulic Engineering, 26(2), pp. 187-197.

12. Hao, B., ShuLiang C., 2014, *Effects of blade rotation angle deviations on mixed-flow pump hydraulic performance,* Sci. China (Tech. Sci.), 57(7), pp. 1372–1382.

13. Hao, B., ShuLiang C., 2013, *Multi-parameter optimization design, numerical simulation and performance test of mixed-flow pump impeller*, Sci. China (Tech. Sci.), 56(09), pp. 2194–2206.

14. Muggli, F.A., Holbein P., Dupont P., 2002, *CFD calculation of a mixed flow pump characteristic from shutoff to maximum flow,* J. Fluids Eng., 124(3), pp. 132–141.

15. Saha, S. L., Kurokawa, J., Matsui, J., Imamura, H., 2000, *Suppression of performance curve instability of a mixed flow pump by use of J-groove*, J. Fluids Eng., 122(3), pp. 592-597.

16. Magnoli, M.V, Giese, M., 2021, *Numerical flow simulation of pump stability for pumped storage units with analysis and visualization of the dynamic flow patterns*, IOP Conference Series: Earth and Environmental Science, 774(1), 012065.

17. Kim, Y.I., Kim, S., Yang, H.M., Lee, K.Y., Choi, Y.S., 2019, *Analysis of internal flow and cavitation characteristics for a mixed-flow pump with various blade thickness effects*, J. Mech. Sci. Tech., 33(7), pp. 3333–3344.

18. Derakhshan, S., Pourmahdavi, M., Abdolahnejad, E., Reihani, A., Ojaghi, A., 2013, *Numerical shape optimization of a centrifugal pump impeller using artificial bee colony algorithm*, Computers & Fluids, 81, pp. 145-151.

19. Kim, S., Choi, Y.S., Lee, K.Y., Kim, J.H., 2011, *Design optimization of mixed-flow pump in a fixed meridional shape*, International journal of fluid machinery and systems, 4(1), pp. 14-24.

20. Kim, S., Lee, K.Y., Kim, J.H., Choi, Y.S., 2014, *A numerical study on the improvement of suction performance and hydraulic efficiency for a mixed-flow pump impeller*, Mathematical Problems in Engineering, 2014, pp. 269-483.

21. Kim, S., Lee, K.Y., Kim, J. H., Kim, J.H., Jung, U.H., Choi, Y.S., 2015, *High performance hydraulic design techniques of mixed-flow pump impeller and diffuser*, Journal of Mechanical Science and Technology, 29, pp. 227-240.

22. Srivastava, S, Apurba, K R, Kaushik, K., 2014, *Design of a mixed flow pump impeller blade and its validation using stress analysis[J]*, Procedia materials science, 6, pp. 417-424.

23. Murillo, O.W., Patiño Arcila, I.D., Palacio-Fernández, J.A., 2022, *Geometric Optimization of Jet Pump Used in Vacuum Distillation Applications under Different Operating Conditions using Genetic-algorithm Methods*, Journal of Applied and Computational Mechanics, 8(1), pp. 340-58.

24. Kim, S., Lee, K. Y., Kim, J. H., Yoon, J. Y., Choi, Y. S., 2018, *Design of mixed-flow pump for Ns475 based on optimum design database*, International Journal of Fluid Machinery and Systems, 11(2), pp. 123-128.

25. Zhao, J., Dong, Y., Fu, J., Zhao, L., Zhang, Y., 2020, *Design and experiment of energy-saving water injection pump*, Journal of Petroleum Exploration and Production Technology, 10(5), pp. 2127-2135.

26. Han, W., Xie, W., Li, R., Wang, H., Pan, Y., Chen, R., Han, J., 2021, *Analysis of influence of guide vane wrap angle and blade number on propulsive performance of a water jet propulsor*, Modern Physics Letters B, 35(33), 2150503.

27. Soto-Valle, R., Gualtieri, M., Bartholomay, S., Manolesos, M., Nayeri, C.N., Bianchini, A., Paschereit, C.O., 2022, *Rotational and blockage effects on a wind turbine model based on local blade forces*, Journal of Physics: Conference Series, 2265(2), 022102.

28. Elsayed, Y., Gabbar, H.A., 2022, *Enhancing FBG Sensing in the Industrial Application by Optimizing the Grating Parameters Based on NSGA-II*, Sensors, 22(21), 8203.

29. Romanova, D., Ivanov, O., Trifonov, V., Ginzburg, N., Korovina, D., Ginzburg, B, Strijhak, S., 2022, *Calibration of the k-ω SST Turbulence Model for Free Surface Flows on Mountain Slopes Using an Experiment*, Fluids, 7(3), 111.

30. Mdee, O. J., Kimambo, C. Z., Nielsen, T. K., Kihedu, J, 2018, *Analytical evaluation of head and flow rate off-design characteristics for pump as turbine application*, Journal of Fluids Engineering, 141(5), 051203.

31. Sritram, P., Suntivarakorn, R., 2021, *The Efficiency Comparison of Hydro Turbines for Micro Power Plant from Free Vortex*, Energies, 14(23), 7961.

32. Azarpira, M., Zarrati, A.R., 2019, *A 3D analytical model for vortex velocity field based on spiral streamline pattern*, Water Science and Engineering, 12(3), pp. 244-252.

33. Sundaravadivelu, K., Absi, R., 2021, *Turbulent kinetic energy estimate in the near wall region of smooth turbulent channel flows*, Meccanica, 56(10), pp. 2533-2545.

34. Yang, Z., Cheng, Y., Liu, K., Hou, X., Zhang, X., Wang, X., Ding, J., 2021, *Three-Dimensional CFD Simulations of Start-Up Processes of a Pump-Turbine Considering Governor Regulation*, Energies, 14(24), 8507..

35. Dong-Ming, L., Xi-Dong, X., 2012, *Application of Energy Conservation for Two Tower Three Pump Technology in Wet Thermal Power*, Thermal Turbine, 41(04), pp. 296-299.